Atmos. Chem. Phys. Discuss., 10, 3301–3318, 2010
www.atmos-chem-phys-discuss.net/10/3301/2010/

Atmospheric
Chemistry
and Physics
Discussions

A comparison of ship and satellite measurements of cloud properties in the southeast Pacific stratus deck

M. A. Brunke[1], **S. P. de Szoeke**[2], **P. Zuidema**[3], **and X. Zeng**[1]

[1]The University of Arizona, Department of Atmospheric Sciences, Tucson, Arizona, USA
[2]Oregon State University, College of Oceanic and Atmospheric Sciences, Corvallis, Oregon, USA
[3]University of Miami, Rosentiel School of Marine and Atmospheric Science, Miami, Florida, USA

Received: 20 October 2009 – Accepted: 12 January 2010 – Published: 8 February 2010

Correspondence to: M. A. Brunke (brunke@atmo.arizona.edu)

Published by Copernicus Publications on behalf of the European Geosciences Union.

Abstract

Here, liquid water path (LWP), cloud fraction, cloud top height, and cloud base height are retrieved by a suite of satellite instruments (the CPR aboard CloudSat, CALIOP aboard CALIPSO, and MODIS aboard Aqua) and compared to ship observations from research cruises made in 2001 and 2003–2007 into the stratus/stratocumulus deck over the southeast Pacific Ocean. It is found that CloudSat LWP is generally too high over this region and the CloudSat/CALIPSO cloud bases are too low which is to be expected from the increased sensitivity to precipitation by both the radar and lidar. This results in a relationship (LWP$\sim h^9$) between CloudSat LWP and CALIPSO cloud thickness (h) that is very different from the adiabatic relationship (LWP$\sim h^2$) from in situ observations. Furthermore, comparing results from a global model (CAM3.1) to ship observations reveals that, while the simulated LWP is quite reasonable, the model cloud is too thick and too low, allowing the model to have LWPs that are almost independent of h. Such differences may be reduced in future versions of both the satellite data and the model.

1 Introduction

Clouds cover a large portion of the Earth while having a profound impact on the Earth's radiative balance and thus also on the climate system's sensitivity to climate forcing. There is a significant scatter in the climate sensitivity between global models that is largely due to uncertainties in cloud processes (Bony et al., 2006 and references therein).

Clouds have long been poorly simulated in models, and among the trickiest clouds to simulate are stratus (St) and stratocumulus (Sc). These clouds cover 34% of the global ocean with some of the greatest amounts in large decks under the influence of subtropical descent over the eastern ocean basins (Klein and Hartmann, 1993). The presence of these clouds has a direct effect on the marine atmospheric boundary layer

(MABL) from entrainment processes linked to the radiative and evaporative cooling at cloud top. These clouds also cool the sea surface which has a direct effect on ocean surface fluxes and thus the MABL as well. The sea surface temperature (SST) bias in the eastern Pacific was reduced by as much as 5 K in a global climate model when a prescribed stratus deck over the Southeast Pacific was included (Ma et al., 1996).

The modeling of St/Sc would benefit from further knowledge of the complex interactions within these clouds. This can be facilitated through aircraft and ship observations of cloud properties such as liquid water path; cloud fraction; and cloud base, top, and thickness. Such measurements were made aboard ship over the Southeast Pacific (SEP) in 2001 and 2003–2008 during the austral spring (October–December) when the St/Sc fraction in this region is the highest (e.g., Bretherton et al., 2004; Kollias et al., 2004; Serpetzoglou et al., 2008; de Szoeke et al., 2009a). These quantities have also been derived from satellite measurements (e.g., Zuidema and Hartmann, 1995) with some of the most recent retrievals from the CloudSat and Cloud-Aerosol Lidar and Infrared Pathfinder Satellite Observations (CALIPSO) satellites.

Here, we compare in situ observations of cloud properties of St/Sc over the Southeast Pacific during cruises from 2001 to 2007 with those obtained from CloudSat, CALIPSO, and the Moderate Resolution Imaging Spectrometer (MODIS). The data are briefly explained in Sect. 2. The results of these comparisons are presented in Sect. 3. We finally summarize the results and briefly apply these data to model evaluation in Sect. 4.

2 Data

The experimental data are summarized in Table 1. Most of the in situ data are from a series of cruises undertaken by the US National Oceanic and Atmospheric Administration (NOAA) R/V Ronald H. Brown into the SEP during the austral spring of 2001 and every spring from 2003–2008 (e.g., de Szoeke et al., 2009a). These are hereafter referred to as the Stratus cruises. These data are available at http://www.esrl.noaa.gov/psd/psd3/synthesis/ and documented in de Szoeke et al. (2009b). The pre-2008 Stratus cruise data are further compared to additional experimental data from the surface and aircraft from the Atlantic Stratocumulus Transition Experiment (ASTEX); the First International Satellite Cloud Climatology Program Regional Experiment (FIRE); the Radiation, Aerosol, and Cloud Experiment (RACE); and the Tropical Instability Wave Experiment (TIWE) as documented in the references listed in Table 1. The cloud properties of interest here are liquid water path (LWP), cloud fraction, cloud base height, and cloud top height. The instruments used to obtain these quantities in the field experiments are summarized in Table 1. Note that the LWPs from the Stratus cruises were physically-derived following Zuidema et al. (2005) with averaging done to minimize occasional uncertain calibration.

Since 2006, data from the Cloud Profiling Radar (CPR) have been available. The CPR is a nadir-viewing space-based 94-GHz radar that is the sole instrument on board CloudSat (Stephens et al., 2008). As part of the A-Train, CloudSat closely follows the Aqua satellite which houses MODIS and the Advanced Microwave Scanning Radiometer-EOS (AMSR-E) and is closely followed by CALIPSO which houses the Cloud-Aerosol Lidar with Orthogonal Polarization (CALIOP) – a nadir-pointing Nd:YAG lidar that produces pulses at 532 and 1064 nm (Winker et al., 2007). The CloudSat Data Processing Centre (http://www.cloudsat.cira.colostate.edu) produces collocated CPR, CALIOP, and MODIS Level 2B data products. Specifically used here are the 2B-CWC-RO for CPR-derived liquid water path, 2B-GEOPROF for MODIS-derived cloud fraction, and 2B-GEOPROF-LIDAR for combined CALIOP- and CPR-derived cloud top and base from the second epoch of Release 4 for October–December from 2006–2008. While we anticipate that the 2B-CWC-RO product would be highly influenced by radar reflectivity's increased sensitivity to droplet size (as described in more detail in the following sections), the single-measurement retrieval is more homogenous than that from another product, the 2B-CWC-RVOD. The latter combines LWP based on the CPR and on MODIS-derived visible cloud optical depths which are unavailable in many situations, most notably at night. CloudSat LWP from 2B-CWC-RO is further intercompared to passive microwave satellite products retrieved from the AMSR-E on Aqua (available at http://nsidc.org/daac/index.html) and the Special Sensor Microwave Imager (SSM/I) aboard the Defense Meteorological Satellite Programme (DMSP) satellites (available at http://www.remss.com) (Wentz, 1997) during October–December 2008.

3 Results

First, LWP from CloudSat, AMSR-E, and SSM/I are compared. CloudSat LWP is higher than that of AMSR-E and SSM/I. SSM/I generally has the lowest LWPs and its mean difference with CloudSat is 87 $\mathrm{g\,m^{-2}}$ with a standard deviation of 191 $\mathrm{g\,m^{-2}}$ for non-zero values in the core of the St/Sc deck (between 12° and 25° S and 70° and 90° W). The mean difference between non-zero CloudSat and AMSR-E values is slightly less at 82 $\mathrm{g\,m^{-2}}$ with a standard deviation of 170 $\mathrm{g\,m^{-2}}$. These differences are further broken down as a function of CloudSat LWP in Fig. 1a. For both day and night passes combined, CloudSat has increasingly higher values than the other two satellites (indicated by the positive differences) except for LWP$<$100 $\mathrm{g\,m^{-2}}$ where CloudSat's LWPs are actually lower than the other two products. The increasingly large differences between CloudSat LWPs and those from the other products are due to the fact that, while all satellites have the most LWPs in the lowest bin ($<$100 $\mathrm{g\,m^{-2}}$), only CloudSat produces LWPs$\geq$500 $\mathrm{g\,m^{-2}}$ (Fig. 1b). This mainly occurs in the nighttime pass, as the median LWP differences are quite similar then to those in Fig. 1a (not shown).

As mentioned in the previous section, some of the above LWP derivations are contaminated by the presence of precipitation (Li et al., 2008). In particular, radar reflectivity is highly sensitive to drop size ($\sim D^6$ where D is drop diameter) (Comstock et al., 2004), thus making radar-derived LWP highly sensitive to the larger precipitation drops. On the other hand, the passive microwave retrievals are relatively insensitive to drop size. To reduce this effect in the radar-derived LWP retrievals, those LWPs that likely include precipitation (whether it is in- or below-cloud) can be excluded. Based on Matrosov et al. (2004), the CloudSat team preliminarily flags possible precipitation for profiles where the maximum reflectivity $Z_{\max} \geq -15\,\mathrm{dBZ}$ (CloudSat Project, available at http://www.cloudsat.cira.colostate.edu/ICD/2B-CWC-RO/2B-CWC-RO_PD_5.1.pdf, 2007). Only 3% of the 937 891 total good-quality profiles are removed in October–December 2008 with this flag, so the differences between the CloudSat averages and the AMSR-E and SSM/I LWPs do not change much. However, Leon et al. (2008) used $Z_{\max} > -18\,\mathrm{dBZ}$ as a criterion in the lowest 4000 m and found a precipitation occurrence of 34% for profiles with cloud top between 1000 and 4000 m in this region. The use of a similar criterion on the CloudSat data used here would eliminate 20% of all good-quality profiles (no matter where the cloud is located) and all LWPs≥500 $\mathrm{g\,m^{-2}}$ (Fig. 1b). The mean difference between non-zero CloudSat and AMSR-E (SSM/I) LWPs reduces to negative values [−65(−62) $\mathrm{g\,m^{-2}}$] with a corresponding decrease in the standard deviation of the differences [55(71) $\mathrm{g\,m^{-2}}$]. There is also some sensitivity to where in the profile $Z_{\max}$ is searched for. For instance, 10% of good-quality profiles have $Z_{\max} > -15\,\mathrm{dBZ}$ in the apparent bottom half of the cloud based on the 2B-GEOPROF product, whereas only 3% have $Z_{\max}$ above that threshold in the apparent top half. Another method to reduce the effect of precipitation is to constrain the radar-derived LWP retrieval by another derivation such as that used in 2B-CWC-RVOD which also uses MODIS-derived visible optical depth to obtain LWP. Future work will investigate the effectiveness of all of these constraints on CloudSat LWPs in this region. However, we retain all good-quality CloudSat profiles here. Thus, part of the differences between the radar-only LWPs and ship LWPs below are due to the effects of precipitation in the radar-derived retrievals.

There are also some substantial differences between the derived quantities from CloudSat, CALIPSO, and MODIS measurements and the Stratus cruise observations. For instance, median CloudSat LWP measurements made in October–December 2006–2008 for ~2.8° latitude and longitude bands are higher than ship observations in the core region of the St/Sc deck (Fig. 2a,d). Again, this is to be expected due to the radar's sensitivity to precipitation, while the retrievals from the passive microwave radiometer aboard the ship would be less sensitive. The CloudSat/CALIPSO cloud top agrees well with ship observations (Fig. 2c,f), but cloud base is lower than observed from the ship (Fig. 2b,e), suggesting that the CloudSat/CALIPSO-derived clouds are too thick in this region. According to Vaughan et al. (2009), the determination of cloud base from lidar attenuation is less straightforward than of cloud top due to the "undetermined" effects of feature attenuation. Plus, the radar-derived cloud bases would be highly affected by the presence of drizzle just like the LWPs are, so this underestimate is likely due to the effects of precipitation in some of the profiles.

These differences are further illustrated by comparing the relationship between cloud thickness (h) and LWP from CloudSat/CALIPSO and the Stratus cruises in Fig. 3a. Some studies showed that liquid water content (LWC) is adiabatic or near-adiabatic within St/Sc (e.g., Albrecht et al., 1990; Zuidema et al., 2005), while others found that LWC can deviate substantially from adiabaticity (e.g., Pawlowska et al., 2000; Zhou et al., 2006). In either case, LWP is directly related to h, as LWP is the integral of LWC over the cloud depth (Zhou et al., 2006):

$$\mathrm{LWP} = \alpha \frac{A}{2} h^2 \quad (1)$$

where A is the adiabatic rate of change with height of LWC and α is the percentage of adiabaticity. Zhou et al. (2006) found a median value for A of $2.24\times10^{-3}\,\mathrm{g\,m^{-4}}$ and a value for α of 0.79. This relationship is shown as the solid line in Fig. 3a, and the Stratus cruise data almost fall onto this line. This is not surprising, as some of the Stratus 2001 data along with the other data from TIWE, FIRE, RACE, and ASTEX were used to derive that relationship. The CloudSat/CALIPSO data, however, have a very different relationship of $\mathrm{LWP}\sim h^9$.

In Fig. 3b, the relationship between observed LWP and cloud fraction is compared to that from CloudSat/MODIS. The ship observations show a somewhat logarithmic increase in median LWP with increasing cloud fraction as in Zhou et al. (2006). However, MODIS cloud fraction is nearly independent of the median CloudSat LWP.

The diurnal cycle of these cloud properties are compared in Fig. 4a–d within 1° of (20° S, 85° W), i.e., the nominal location of the buoy operated by the Woods Hole Oceanographic Institution. The ship-observed hourly median of 10-min LWP has a maximum of 154 g m^{-2} in the early morning (at 05:00 LT) and a minimum of 35 g m^{-2} in the afternoon (at 13:00 LT) (Fig. 4a) quite similar to the diurnal cycle obtained from all ship observations during Stratus 2001 only (Zuidema et al., 2005, Fig. 10). The median cloud fraction is less than 1 only between 10:00 and 16:00 LT with values as low as 0.95 (Fig. 4b). Ship cloud base and top change little throughout the day with a difference of only 150 m and 126 m, respectively, between their maxima and minima (Fig. 4c, d).

Because of the sun-synchronous orbits of their satellites, CloudSat/CALIPSO/MODIS values can only be obtained at this site twice during the mean diurnal cycle. CloudSat LWP is lower in the day than at night which is consistent with the ship observations. As expected from the increased sensitivity of the radar and lidar to precipitation, the satellite-derived LWP values are higher than the ship data (by 157 g m^{-2} at night and 104 g m^{-2} in the day, Fig. 4a), and CALIPSO cloud base is lower than the ship observations (by 502 m at night and 312 m in the daytime) with a slightly higher diurnal cycle than the ship with a difference between the daytime and nighttime passes of 210 m (Fig. 4c). In contrast, CALIPSO cloud top is closer to the ship-observed values (302 m higher at night and 66 m lower in the day) but has a higher difference between passes (345 m, Fig. 4d).

The satellite cloud properties are further compared with the ship observations at (20° S, 75° W), a location closer to the coast near the Chilean Servicio Hidrográfico y Oceanográfico de la Armada (SHOA) buoy (Fig. 4e–h). Here, the ship observations within 1° of this location show a somewhat similar diurnal cycle to that at the western location with a maximum LWP at 05:00 LT and a minimum LWP at 14:00 LT (Fig. 4e). The ship observations here also exhibit a secondary maximum in the evening (20:00 LT) which is consistent with previous findings from satellite retrievals in the region (O'Dell et al., 2008). There are more hours with complete cloud cover at this location with only two hours (15:00–16:00 LT) of median cloud fraction<1 (Fig. 4f). Again, cloud base does not change very much over the course of the day (Fig. 4g), but cloud top has a little more variability with a difference of 257 m between the minimum in the afternoon (15:00 LT) and the maximum in the morning (08:00 LT) (Fig. 4h).

CloudSat measurements of LWP within 1° of (20° S, 75° W) are closer to the ship observations here (Fig. 4e) than at 85° W. As at 85° W, CALIPSO cloud top compares well with the ship (Fig. 4h), but again CALIPSO cloud base is too low, particularly at night (Fig. 4g).

4 Conclusions

Some differences in the collocated CloudSat, CALIPSO, and MODIS measurements of cloud properties have been found here in the SEP St/Sc deck when compared to those from other satellite products and ship observations. For instance, the clouds as measured by CloudSat and CALIPSO are on average too thick, because the cloud bases are too low compared to ship observations (Figs. 2 and 4). Also, CloudSat LWP is also on average higher than ship observations and passive microwave satellite measurements over this region (e.g., Figs. 1–2). These differences in cloud thickness result in a very different relationship between LWP and h from CloudSat/CALIPSO (LWP$\sim h^9$) as opposed to that from in situ observations (LWP$\sim h^2$, Fig. 3a). These overestimates in radar-derived LWP and underestimates in cloud base derived from both the radar and lidar are to be expected due to increased sensitivity to precipitation. Such effects are reduced in LWP closer to the coast (at 75° W vs. at 85° W, e.g., Fig. 4e vs. 4a) where precipitation occurrence is reduced (Leon et al., 2008, Fig. 4a). Such effects would also be reduced by eliminating probable precipitating profiles based on the maximum reflectivity, Z_{max}. The current CloudSat flag based on $Z_{\text{max}} \geq -15$ dBZ only removes 3% of the good-quality profiles in October–December 2008, whereas a lower threshold ($Z_{\text{max}} > -18$ dBZ) searched for in the lowest 4000 m (Leon et al., 2008) eliminates more (20%). There is also some sensitivity to where the thresholding is taking place, as more profiles have $Z_{\text{max}} > -15$ dBZ in the apparent bottom half of the cloud (10%) versus the 3% that is in the apparent upper half.

The ship and satellite measurements both show a clear diurnal cycle at (20° S, 85° W) with maximum LWP and CF at night and minimum in these quantities during the day (Fig. 4a–b). A similar diurnal cycle exists in the ship and satellite measurements at the SHOA buoy site closer to the coast (Fig. 4e–f).

An important motivation of these data analyses is the use of these data for model evaluation. We have used these data to preliminarily evaluate the performance of the Community Atmosphere Model (CAM3.1). Figure 3a shows that CAM3.1 has LWPs that are nearly independent of h. Since model LWP is comparable to the ship observations (Fig. 2a, d), this is likely due to the simulated cloud being too thick and too low (Fig. 2b, c, e, f). However, the model is able to produce a logarithmic relationship between LWP and cloud fraction similar to that of the ship observations that does not appear in the satellite data (Fig. 3b). Additionally, CAM3.1 is able to correctly capture the diurnal cycle at (20° S, 85° W) but has an opposite diurnal cycle at (20° S, 75° W) (Fig. 4). Such discrepancies have also been seen in other models (e.g., Duynkerke and Teixeira, 2001; Siebesma et al., 2004).

These analyses also provide a context for the interpretation of the work in the other papers in this Variability of the American Monsoon Systems Ocean Cloud Atmosphere Land Study (VOCALS) special issue. It is recognized that both the satellite datasets and the model are continually being updated, so future work which will include data from the recent VOCALS Regional Experiment conducted in October–November 2008 will analyze any updated versions of the CloudSat collocated data as well as simulations from the soon-to-be-released CAM4.

Acknowledgement. This study was supported by the NSF (ATM0745661). J. Teixeira and an anonymous reviewer are thanked for their helpful comments. We also sincerely appreciate the numerous groups involved in the development of the various satellite and ship- and aircraft-based datasets used in this study.

References

Albrecht, B. A., Fairall, C. W., Thomson, D. W., White, A. B., Snider, J. B., and Schubert, W. H.: Surface-based remote sensing of the observed and the adiabatic liquid water content of stratocumulus clouds, Geophys. Res. Lett., 17, 89–92, 1990.

Austin, P., Wang, Y., Pincus, R., and Kujula, V.: Precipitation in stratocumulus clouds: Observational and modeling results, J. Atmos. Sci., 52, 2329–2352, 1995.

Bony, S., Colman, R., Kattsov, V. M., Allan, R. P., Bretherton, C. S., Dufresne, J., Hall, A., Hallegatte, S., Holland, M. M., Ingram, W., Randall, D. A., Soden, B. J., Tselioudis, G., and Webb, M. J.: How well do we understand and evaluate climate change feedback processes?, J. Climate, 19, 3445–3482, 2006.

Bretherton, C. S., Uttal, T., Fairall, C. W., Yuter, S. E., Weller, R. A., Baumgardner, D., Comstock, K., Wood, R., and Raga, G. B.: The EPIC 2001 stratocumulus study, B. Am. Meteorol. Soc., 85, 967–977, 2004.

Comstock, K. K., Wood, R., Yuter, S. E., and Bretherton, C. S.: Reflectivity and rain rate in and below drizzling stratocumulus, Q. J. Roy. Meteor. Soc., 130, 2891–2918, 2004.

de Szoeke, S. P., Fairall, C. W., and Pezoa, S.: Ship observations of the tropical Pacific Ocean along the coast of South America, J. Climate, 22, 458–464, 2009a.

de Szoeke, S. P., Fairall, C. W., Wolfe, D. E., Bariteau, L., and Zuidema, P.: Surface flux observations on the southeastern tropical Pacific Ocean and attribution of SST errors in coupled ocean-atmopshere models, submitted, J. Climate, 2009b.

Duynkerke, P. G. and Teixeira, J.: Comparison of the ECMWF reanalysis with FIRE I observations: Diurnal variation of marine stratocumulus, J. Climate, 14, 1466–1478, 2001.

Klein, S. A. and Hartmann, D. L.: The seasonal cycle of low stratiform clouds, J. Climate, 6, 1587–1606, 1993.

Kollias, P., Fairall, C. W., Zuidema, P., Tomlinson, J., and Wick, G. A.: Observations of marine stratocumulus in SE Pacific during the PACS 2003 cruise, Geophys. Res. Lett., 31, L22110, doi:10.1029/2004GL020751, 2004.

Leon, D. C., Wang, Z., and Liu, D.: Climatology of drizzle in marine boundary layer clouds based on 1 year of data from CloudSat and Cloud-Aerosol Lidar and Infrared Pathfinder Satellite Observations (CALIPSO), J. Geophys. Res., 113, D00A14, doi:10.1029/2008JD009835, 2008.

Li, J.-L. F., Waliser, D., Woods, C., Teixeira, J., Bacmeister, J., Chern, J., Shen, B.-W., Tompkins, A., Tao, W.-K., and Köhler, M.: Comparisons of satellites liquid water estimates to ECMWF and GMAO analyses, 20th century IPCC AR4 climate simulations, and GCM simulations, Geophys. Res. Lett., 35, L19710, doi:10.1029/2008GL035427, 2008.

Ma, C.-C., Mechoso, C. R., Robertson, A. W., and Arakawa, A.: Peruvian stratus clouds and the tropical Pacific circulation: a coupled ocean-atmosphere GCM study, J. Climate, 9, 1635–1645, 1996.

Matrosov, S. Y., Uttal, T., and Hazen, D. A.: Evaluation of radar reflectivity-based estimates of water content in stratiform marine clouds, J. Appl. Meteorol., 43, 405–419, 2004.

O'Dell, C. W., Wentz, F. J., and Bennartz, R.: Cloud liquid water path from satellite-based passive microwave observations: a new climatology over the global oceans, J. Climate, 21, 1721–1739, 2008.

Pawlowska, H., Brenguier, J. L., and Burnet, F.: Microphysical properties of stratocumulus clouds, Atmos. Res., 55, 15–33, 2000.

Räisänen, P., Isaac, G. A., Barker, H. W., and Gultepe, I.: Solar radiative transfer for stratiform clouds with horizontal variations in liquid-water path and droplet effective radius, Q. J. Roy. Meteor. Soc., 129, 2135–2149, 2003.

Serpetzoglou, E., Albrecht, B. A., Kollias, P., and Fairall, C. W.: Boundary layer, cloud, and drizzle variability in the southeast Pacific stratocumulus regime, J. Climate, 21, 6191–6214, 2008.

Siebesma, A. P., Jakob, C., Lenderink, G., Neggers, R. A. J., Teixeira, J., Van Meijgaard, E., Calvo, J., Chlond, A., Grenier, H., Jones, C., Kohler, M., Kitagawa, H., Marquet, P., Lock, A. P., Muller, F., Olmeda, D., and Severijns, C.: Cloud representation in general-circulation models over the Northern Pacific Ocean: a EUROCS intercomparison study, Q. J. Roy. Meteor. Soc., 130, 3245–3267, 2004.

Stephens, G. L., Vane, D. G., Tanelli, S., Im, E., Durden, S., Rokey, M., Reinke, D., Partain, P., Mace, G. G., Austin, R., L'Ecuyer, T., Haynes, J., Lebsock, M., Suzuki, K., Waliser, D., Wu, D., Kay, J., Gettelman, A., Wang, Z., and Marchand, R.: CloudSat mission: performance and early science after the first year of operation, J. Geophys. Res., 113, D00A18, doi:10.1029/2008JD009982, 2008.

Vaughan, M. A., Powell, K. A., Kuehn, R. E., Young, S. A., Winker, D. M., Hostetler, C. A., Hunt, W. H., Liu, Z., McGill, M. J., and Getzewich, B. J.: Fully automated detection of cloud and aerosol layers in the CALIPSO lidar measurements, J. Atmos. Ocean. Technol., 26,

Title Page
Abstract | Introduction
Conclusions | References
Tables | Figures
◂◂ | ▸▸
◂ | ▸
Back | Close
Full Screen / Esc
Printer-friendly Version
Interactive Discussion

2034–2050, 2009.

Wentz, F. J.: A well-calibrated ocean algorithm for special sensor microwave/imager, J. Geophys. Res., 102, 8703–8718, 1997.

White, A. B., Fairall, C. W., and Snider, J. B.: Surface-based remote sensing of marine boundary-layer cloud properties, J. Atmos. Sci., 52, 2827–2838, 1995.

Winker, D. M., Hunt, W. H., and McGill, M. J.: Initial performance assessment of CALIOP, Geophys. Res. Lett., 34, L19803, doi:10.1029/2007GL030135, 2007.

Wood, R. and Field, P. R.: Relationships between total water, condensed water, and cloud fraction in stratiform clouds examined using aircraft data, J. Atmos. Sci., 57, 1888–1905, 2000.

Zhou, M., Zeng, X., Brunke, M., Zhang, Z., and Fairall, C.: An analysis of statistical characteristics of stratus and stratocumulus over Eastern Pacific, Geophys. Res. Lett., 33, L02807, doi:10.1029/2005GL024796, 2006.

Zuidema, P. and Hartmann, D. L.: Satellite determination of stratus cloud microphysical properties, J. Climate, 8, 1638–1657, 1995.

Zuidema, P., Westwater, E. R., Fairall, C., and Hazen, D.: Ship-based liquid water path estimates in marine stratocumulus. J. Geophys. Res., 110, D20206, doi:10.1029/2005JD005833, 2005.

Table 1. In situ data used in this study. See the text for the meaning of the experiment acronyms.

Experiment	Reference(s)	Year(s)	Location	Instrumentation for acquiring			
				Liquid water path	Cloud fraction	Cloud base	Cloud top
Ship/Surface							
Stratus cruises	Bretherton et al. (2004), Kollias et al. (2004), Serpetzoglou et al. (2008), de Szoeke et al. (2009a)	2001, 2003–2007	SE Pacific	MWR	ceilo.	ceilo.	MMCR
ASTEX	White et al. (1995)	1992	N Atlantic	MWR	ceilo.	ceilo.	915-MHz radar
TIWE	White et al. (1995)	1991	Eq. Central Pacific	ceilo., 915-MHz radar	ceilo.	ceilo.	915-MHz radar
Aircraft							
RACE	Räisänen et al. (2003)	1995	Canada	FSSP, hot wire probe			
ASTEX	Wood and Field (2000)	1992	N Atlantic	Hot wire probe			
FIRE	Austin et al. (1995)	1987	NE Pacific	FSSP, 260X			

MWR = microwave radiometer, ceilo. = ceilometer, MMCR = millimeter-wave cloud radar, FSSP = forward scattering spectrometer probe, 260X = optical array probe.

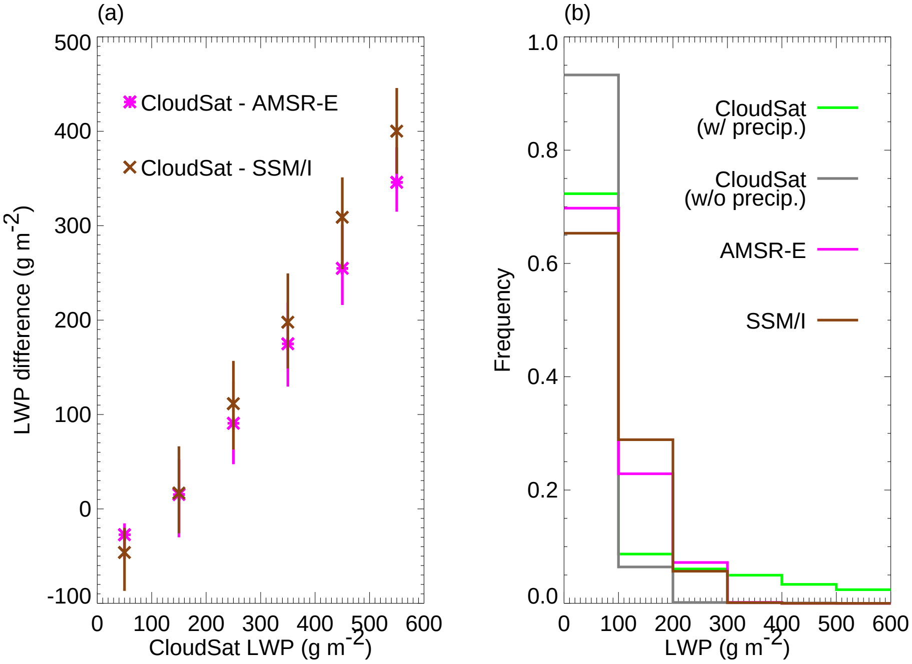

Fig. 1. **(a)** The median difference between liquid water path (LWP) from CloudSat averaged over 0.25°×0.25° grid boxes within 12°–25° S and 70°–90° W in October–December 2008 and that of AMSR-E and SSM/I for 100 g m^{-2} bins of CloudSat LWP. **(b)** The frequency distribution of LWP for each satellite per 100 g m^{-2} bin.

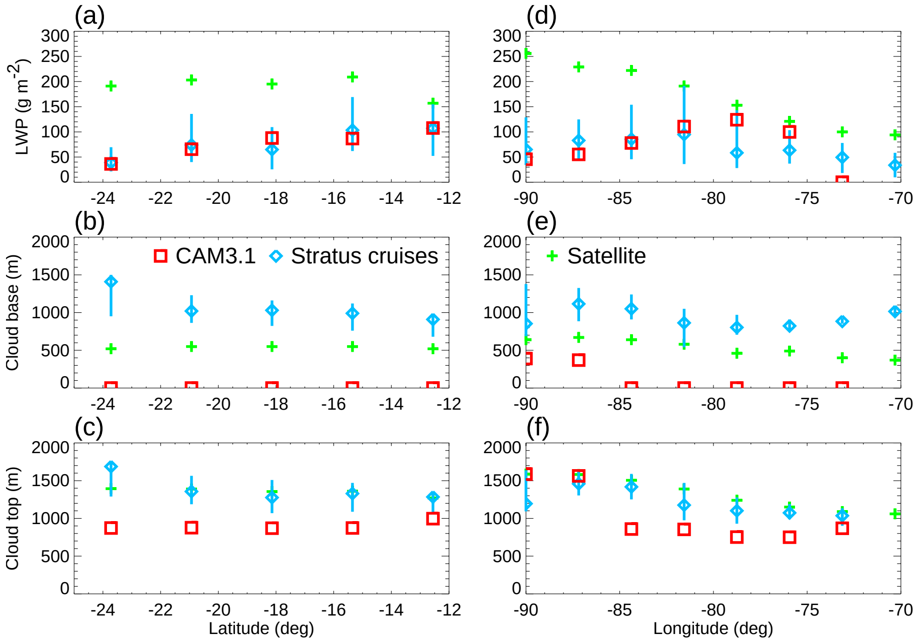

Fig. 2. Median (**a** and **d**) LWP, (**b** and **e**) cloud base height, and (**c** and **f**) cloud top height for ~2.8° latitude **(a–c)** and longitude **(d–f)** bands from the 2001–2007 Stratus cruises (with the interquartile ranges indicated by the vertical lines); satellite data (from CloudSat, MODIS, or CALIPSO); and the Community Atmosphere Model (CAM3.1).

Title Page
Abstract
Introduction
Conclusions
References
Tables
Figures
◀|
|▶
◀
▶
Back
Close
Full Screen / Esc
Printer-friendly Version
Interactive Discussion

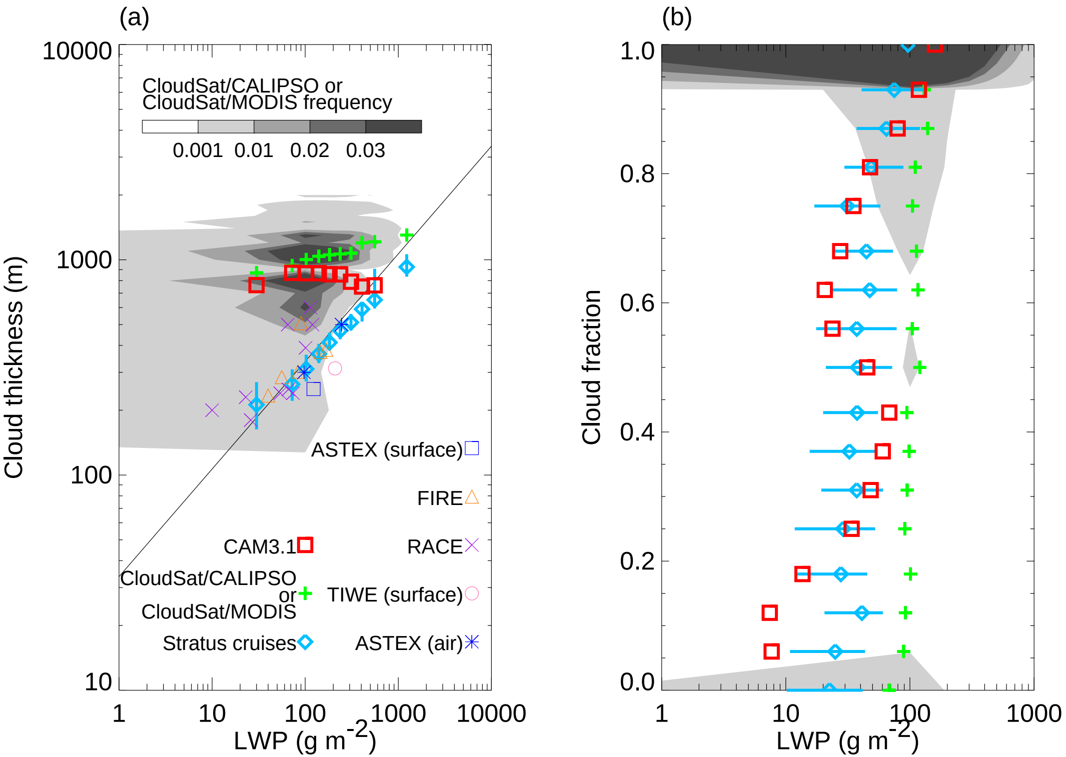

Fig. 3. **(a)** Median cloud thickness for LWP bins of varying size from the Stratus cruises (with the interquartile ranges indicated by the vertical lines), CloudSat/CALIPSO, and CAM3.1 along with values derived from various other field experiments. Also shown is the frequency distribution of CloudSat LWP/CALIPSO thickness data pairs. The thin line is the fit to Eq. (1). **(b)** Median LWP for cloud fraction bins of varying size from the Stratus cruises (with the interquartile ranges indicated by the horizontal lines), CloudSat/MODIS, and CAM3.1 along with the frequency distribution of CloudSat LWP/MODIS cloud fraction data pairs.

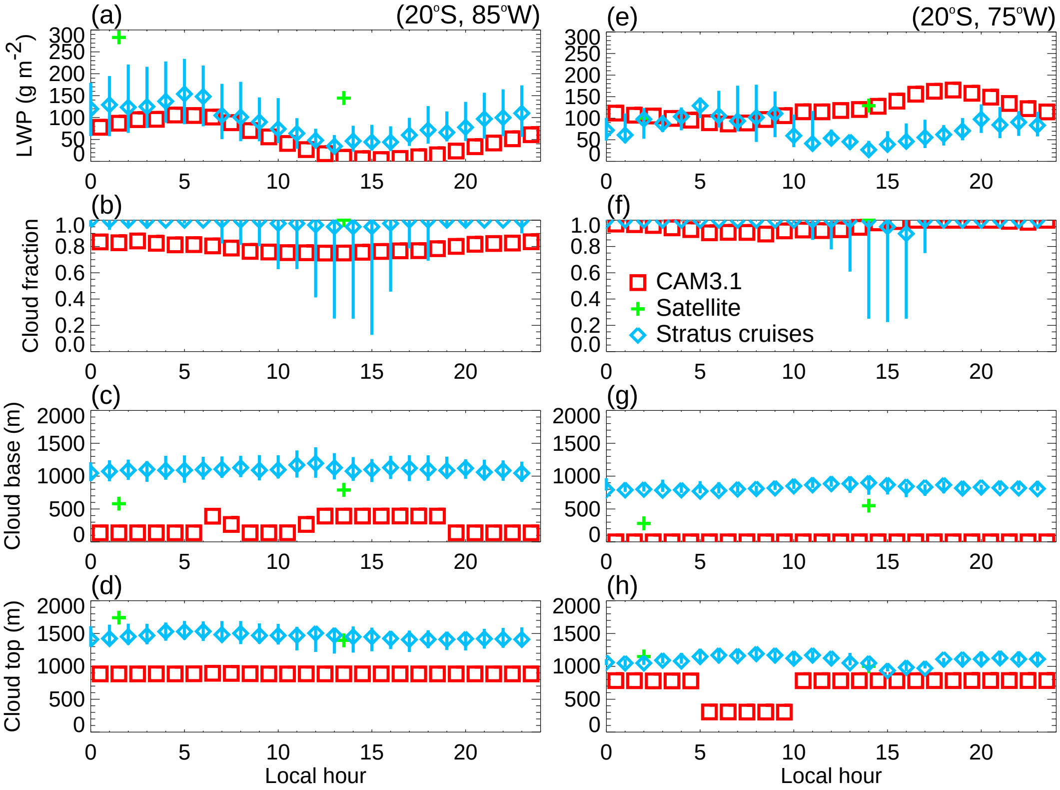

Fig. 4. Median hourly (**a** and **e**) LWP, (**b** and **f**) cloud fraction, (**c** and **g**) cloud base, and (**d** and **h**) cloud top at (20° S, 85° W) **(a–d)** and at (20° S, 75° W) **(e–h)** from the 2001–2007 Stratus cruises (with the interquartile ranges indicated by the vertical lines); satellite data (from CloudSat, MODIS, or CALIPSO); and CAM3.1.